THE JOURNAL OF BIOLOGICAL CHEMISTRY
Vol. 279, No. 7, Issue of February 13, pp. 5829–5836, 2004

Printed in U.S.A.

The Human Amyloid-β Precursor Protein$_{770}$ Mutation V717F Generates Peptides Longer Than Amyloid-β-(40–42) and Flocculent Amyloid Aggregates*

Received for publication, October 16, 2003, and in revised form, November 21, 2003
Published, JBC Papers in Press, November 26, 2003, DOI 10.1074/jbc.M311380200

Alex E. Roher‡§, Tyler A. Kokjohn¶, Chera Esh‡, Nicole Weiss‡, Jennifer Childress‡, Walter Kalback‡, Dean C. Luehrs‡, John Lopez‖, Daniel Brune‖, Yu-Min Kuo, Martin Farlow§§, Jill Murrell§§, Ruben Vidal§§, and Bernardino Ghetti§§**

*From the ‡The Longtine Center for Molecular Biology and Genetics, Sun Health Research Institute, Sun City, Arizona 85351, ¶Department of Microbiology, Midwestern University, Glendale, Arizona 85308, ‖Department of Chemistry and Biochemistry, Arizona State University, Tempe, Arizona 85287, **Department of Cell Biology and Anatomy, National Cheng Kung University, Tainan, Taiwan 701, and §§Indiana Alzheimer Disease Center, Indianapolis, Indiana 46202*

One of the familial forms of Alzheimer's disease (AD) encodes the amyloid-β precursor protein (AβPP) substitution mutation V717F. This mutation is relevant to AD research, since it has been utilized to generate transgenic mice models to study AD pathology and therapeutic interventions. Amyloid beta (Aβ) peptides were obtained from the cerebral tissue of three familial AD subjects carrying the AβPP V717F mutation. A combination of ultracentrifugation, size-exclusion, and reverse-phase high performance liquid chromatography, tryptic and cyanogen bromide hydrolysis, amino acid analysis, and matrix-assisted laser desorption ionization and surface-enhanced laser desorption ionization mass spectrometry was used to characterize the familial AD mutant Aβ peptides. The AβPP V717F mutation, located 4–6 residues beyond the wild-type AβPP γ-secretase cleavage site, yielded longer Aβ peptides with C termini between residues 43 and 54. In the cerebral cortex these peptides aggregated into thin water- and SDS-insoluble amyloid bundles that condensed into flocculent spherical plaques. In the leptomeningeal arteries the amyloid was deposited in moderate amounts and was primarily composed of the shorter and more soluble Aβ species ending at residues 40, 42, and 44. The single V717F mutation in AβPP results in distinctive and drastic changes in the length and tertiary structure of Aβ peptides, which appear to be responsible for the earlier clinical manifestations of dementia and death of these patients.

Alzheimer's disease (AD)[1] is characterized by profuse amyloid fibril deposition in cortical neuritic plaques and cerebral vessel walls (1). The amyloid-β (Aβ) peptides consist predominately of 40–42 amino acid residues derived from amyloid-β precursor protein (AβPP) proteolysis. Rare, familial mutations both within the Aβ coding domain and flanking N- and C-terminal regions have been described that result in Aβ deposition, dementia, and in some cases hemorrhagic stroke (2, 3). In addition, mutations in the presenilin 1 and 2 genes also produce the characteristic neuropathological lesions and clinical expression of AD dementia (3, 4). Despite the fact that familial AD (FAD) patients reproduce many of the same characteristic features prominent in sporadic AD, the vast majority of dementia cases do not possess any obvious genetic basis.

One of the best characterized forms of FAD is the Val → Phe mutation at position 717 of the AβPP (AβPP$_{770}$ isoform numbering), a rare mutation expressed in a single family (5). Neurological disease is clinically manifested in relatively young individuals who become demented in their late thirties to early forties and die at about fifty years of age (6, 7). This mutation is of great biological importance since it has been utilized to construct an AβPP transgenic (Tg) mouse in combination with the platelet-derived growth factor promoter to enhance Aβ production and amyloid deposition (8, 9). Known as the PDAPP Tg mouse, the model is widely employed in academic and industrial settings to study fundamental Aβ peptide chemistry and amyloid pathophysiology (8). The PDAPP Tg mice reproduce some of the pathological features observed in AD such as senile plaques with amyloid cores, dystrophic neurites, synaptic loss, astrogliosis, and microgliosis but lack any detectable neurofibrillary tangle pathology (10).

Morphologically, three unique pathological features distinguish AβPP V717F individuals from sporadic AD cases, 1) the generation of flocculent amyloid plaques, 2) an almost complete absence of compact amyloid cores, and 3) an enormous production of neurofibrillary tangles (NFT). The extreme scarcity of AβPP V717F individuals has precluded a biochemical comparison between the amyloid peptides deposited in these FAD cases and those present in sporadic AD. Because several important AβPP Tg mice models employ this specific mutation to mimic AD amyloid production and deposition, it is critical to establish the precise chemical nature of the Aβ peptides in both humans and AβPP Tg mice.

We characterized the Aβ-related peptides derived from three FAD individuals carrying the AβPP V717F mutation and compared them to the Aβ peptides characteristic of sporadic AD patients. Our experiments revealed that the biochemical and pathological attributes of AβPP V717F FAD amyloid differ

* This study was supported in part by the State of Arizona Alzheimer's Disease Research Center and by National Institutes of Health Grants AG-19795, AG-10133, and AG-17490. The costs of publication of this article were defrayed in part by the payment of page charges. This article must therefore be hereby marked "*advertisement*" in accordance with 18 U.S.C. Section 1734 solely to indicate this fact.

§ To whom correspondence should be addressed: Sun Health Research Institute, 10515 W. Santa Fe Dr., Sun City, AZ 85351. Tel.: 623-876-5465; Fax: 623-876-5698; E-mail: alex.roher@sunhealth.org.

[1] The abbreviations used are: AD, Alzheimer's disease; Aβ, amyloid-β; AβPP, Aβ precursor protein; FAD, familial Alzheimer's disease; FPLC, fast performance liquid chromatography; GDFA, glass-distilled formic acid; HPLC, high performance liquid chromatography; MALDI-TOF, matrix-assisted laser desorption ionization time-of-flight; NFT, neurofibrillary tangles; SELDI-TOF, surface-enhanced laser desorption ionization time-of-flight; TBS, Tris-buffered saline; Tg, transgenic; Tp, tryptic; TBS-T, TBS with Tween 20; PBS, phosphate-buffered saline.

significantly from those characteristic of sporadic AD. The presence of the AβPP Phe substitution at position Aβ46 (Aβ numbering) 4–6 amino acids beyond the normal Aβ peptide wild-type C-terminal Ala-42 or Val-40 residues results in the generation of longer and more hydrophobic Aβ peptides than those that exist in sporadic AD patients. These extended-length Aβ peptides are associated with clinical and pathological manifestations vastly different from sporadic AD.

MATERIALS AND METHODS

Human Subjects—All three subjects investigated in the present report were demented, belonged to the same family, and were heterozygous for the FAD autosomic dominant Val → Phe mutation at position 717 of the $A\beta PP_{770}$. A complete description of the family pedigree is given in Farlow et al. (6). Patient A, a female, was diagnosed with AD at age 43 and died at age 53. Patient B, a male, was diagnosed with AD at age 39 and died at age 45. Patient C, a female, was diagnosed with AD at age 40 and died at age 49. The brain regions used in this study were frontal and parietal cortex (patient A), superior and middle frontal gyri (patient B), and occipital leptomeninges (patient C). The postmortem delays were 19, 4, and 3 h for patients A, B, and C, respectively. All three patients were homozygous for apolipoprotein E ϵ3.

Isolation of Parenchymal Amyloid—Approximately 10 g of cerebral cortex from patient A and 13 g from patient B were dissected from underlying white matter. The leptomeninges overlying the cerebral cortex were removed, and the gray matter was minced and divided into two equal portions that were subjected to two different amyloid purification protocols.

Protocol A—The gray matter was homogenized in 10 volumes of TBS buffer (0.1 M Tris-HCl, 2 mM EDTA, pH 7.5, 1% SDS) to which 1 tablet of enzyme inhibitors (Roche Diagnostics) per 100 ml of buffer was added. An equal volume of a 4% SDS solution prepared in the same buffer was added to yield a final concentration of 2.5%. After 4 h of gentle stirring, the homogenate was filtered through a 100-μm nylon mesh to eliminate most of the larger blood vessels and centrifuged 2 h at 135,000 × *g* (Beckman SW 28 rotor) at 20 °C. The resulting pellets were suspended in 100 ml of TBS buffer and passed through a 50-μm nylon mesh, and the filtrate was centrifuged at 1000 × *g* for 10 min. This pellet contained a large amount of smaller blood vessels and NFT. The supernatant was centrifuged for 2 h at 275,000 × *g* (Beckman SW 41 rotor), and the supernatant was filtered through a 37-μm nylon mesh. The pellets were suspended, and washed with 10 ml of distilled water, and centrifuged at 275,000 × *g* for 30 min. The final pellets were dissolved in 10 ml of 90% glass-distilled formic acid (GDFA), divided into in 500-μl samples, and centrifuged at 480,000 × *g* for 15 min (Beckman TLA 120.2 rotor). The supernatants were stored at −85 °C and subsequently chromatographed at room temperature on a FPLC Superose 12 size-exclusion column (1 × 30 cm, Amersham Biosciences) in the presence of 80% GDFA at a flow rate of 15 ml/h and monitored at 280 nm. Fractions corresponding to the 2.5–9-kDa mass range were collected and pooled followed by the addition of 5 μl of 2% aqueous betaine (Sigma). The FPLC columns had been previously calibrated using a reversed Aβ amino acid sequence (Aβ residues 40–1).

Protocol B—Approximately 13 g of cerebral cortex was dissolved in 66 ml of 90% GDFA and thoroughly dissolved using a glass homogenizer. The lysed tissue was loaded into 6 polyallomer tubes (14 × 89 mm) and centrifuged at 275,000 × *g* (Beckman SW 41 rotor) for 1 h at 10 °C. The thick fatty layer floating at the top of the tube was carefully avoided, and the supernatant was removed by aspiration while also avoiding the small pellet at the bottom of the tube. The supernatant was divided into 500-μl aliquots and submitted to FPLC using the conditions described for Protocol A. Fractions encompassing a 2.5–9.0-kDa mass range were collected, and volumes were reduced by vacuum centrifugation to ~50 μl and stored at −85 °C.

Isolation of Leptomeningeal Vascular Amyloid—The leptomeninges were gently separated from the brain surface of patient C and washed extensively with cold distilled water to eliminate all traces of blood. During this process vessels larger than 500 μm in diameter were dissected and eliminated since in our experience they do not contain detectable thioflavine S staining cerebrovascular amyloid deposits (11). The washed leptomeningeal vessels were finely minced and submitted to 90% GDFA extraction and disruption in a glass homogenizer, which was followed by sieving through a nylon mesh (37 μm). The resulting filtrate was centrifuged at 275,000 × *g* for 1 h at 10 °C, and the supernatant was subjected to FPLC following the protocol described above.

High Performance Liquid Chromatography (HPLC)—The FPLC fractions containing the Aβ peptides were further separated on a Thermo Separation Products HPLC (Schaumburg, IL) using a Zorbax 300 SB C8 column (300-Å pore, 5-μm particle size, 6.4 × 250 mm; Mac-Mod, Chadds Ford, PA) employing a 2-solvent system (A: water, 0.1% trifluoroacetic acid; B: acetonitrile, 0.1% trifluoroacetic acid). The column was equilibrated with 20% solvent B. For a single HPLC experiment, 5 FPLC runs, each reduced to a volume of ~50 μl, were pooled, and 100 μl of 80% GDFA (to enhance solubility) and 150 μl of water were added just before loading onto the column (total of 500 μl of loading loop capacity). The chromatography was developed with a linear gradient as follows: 0–15 min at 20% B; 16–75 min at 20–40% B; 76–135 min at 40–100% B. During the whole procedure the column was maintained at a constant temperature of 80 °C using an LKB 2155 column oven (Amersham Biosciences). Chromatographic separations were followed by monitoring UV absorbance at 214 nm.

Immuno Dot Blot—A polyvinylidene difluoride membrane was soaked in methanol for 10 s, then immersed in TBS-T (50 mM Tris, pH 7.6, 0.9% NaCl, 0.05% Tween 20) and sandwiched between a multiwell bio-dot blot apparatus (Bio-Rad) connected to a vacuum line. Into each of the wells 450 μl of each of the collected FPLC or HPLC fractions was deposited, and the fluid was removed by vacuum. The membrane was blocked with 5% milk in TBS (50 mM Tris, pH 7.6, 0.9% NaCl) for 1 h at 4 °C and then incubated at room temperature with a 1:500 dilution of the anti-Aβ antibodies 4G8 and 6E10 (Signet, Dedham, MA) for 2 h and rinsed 6 times with TBS-T and 2 times with TBS. The membrane was then incubated with 1:10,000 dilution of goat anti-mouse IgG (Pierce). After repeating the washes as indicated above, the reactive proteins were visualized with the enhanced chemiluminescence detecting reagents (Amersham Biosciences) following the steps indicated by the manufacturer.

Enzymatic Digestion and Cyanogen Bromide Cleavage—The chromatographic fractions containing Aβ peptides that were separated by high temperature HPLC were pooled from several runs and concentrated by vacuum centrifugation to an ~1-ml volume. The specimens were dialyzed (SpectraPor 6 membrane 2000-Da cutoff) against water for 1 h followed by 2 changes of 0.1 M ammonium bicarbonate. Once equilibrated, the specimens were digested with freshly prepared trypsin (~10 μg/ml) for 16 h at 37 °C. To minimize hydrophobic peptide losses, all the fractionated peptides were collected and hydrolyzed in polypropylene tubes. To facilitate the separation of long nonpolar peptides and reduce hydrophobicity, the Aβ peptides were further cleaved at Met residues by cyanogen bromide (CNBr) in the presence of 80% GDFA for 16 h at room temperature. The volumes of the resulting tryptic- and CNBr-digested peptides were subsequently reduced in a rotary evaporator. Peptides were separated by HPLC using the same equipment as above on a Zorbax C8 SB (300-Å pore, 5-μm particle size, 6.4 × 250 mm; Mac-Mod) column at room temperature using a 2-solvent system (A: water, 0.1% trifluoroacetic acid; B: acetonitrile, isopropanol (1:2 volume/volume) containing 0.1% trifluoroacetic acid). After equilibration with solvent A, the chromatographs were developed with a linear gradient, 0–15 min at 0% B, 16–60 min at 0–15% B, 61–130 min at 15–55% B, and monitored at 214 nm.

Automated Amino Acid Analysis—Selected HPLC-separated peptides were submitted to automated amino acid analysis. The peptides were hydrolyzed in the presence of 6 M glass-distilled HCl, 0.1% phenol in a gas phase Waters PicoTag work station hydrolysis unit (Walters, Milford, MA) at 150 °C for 90 min. After removal of the acid by vacuum centrifugation the specimens were transferred into an automatic sample loader unit attached to a Thermo Separation Products HPLC (Schaumburg, IL), and the amino acids were separated on a sodium cation exchange column. The amino acids were detected using a Pickering Laboratories Model PCX-5200 post-column ninhydrin derivatization (Model PCX-5200 Pickering Laboratories, Mountain View, CA), recorded at 570 and 440 nm and automatically quantified against amino acid standards.

Mass Spectrometry—Two different mass spectrometric technologies were employed to determine the M_r of the HPLC-separated peptides. Some of the HPLC-separated fractions were subjected to a Vestec Lasetec mass spectrometer equipped with a nitrogen laser that produced 337-nm pulses of 3 ns duration at a repetition rate of ~7 Hz. Mass spectra were acquired in the positive ion mode. HPLC-purified peptide samples were mixed with an equal volume of a saturated α-cyano-4-hydroxycinnamic acid solution dissolved in a 1:1 mixture of 0.1% trifluoroacetic acid in water and acetonitrile, and 1 μl of the mixture was dried on a stainless steel sample pin. Each mass spectrum was the average of 128 laser shots. Calibration was performed using two synthetic peptides (protonated average masses of 568.696 and 1980.238) as

external standards. Monoisotopic masses obtained by this procedure are accurate to within 1 Da over the mass range of peptides examined in this work.

HPLC peaks were also analyzed by surface-enhanced laser desorption ionization time of flight (SELDI-TOF) mass spectrometry (Ciphergen Biosystems Inc., Palo Alto, CA). The anti-Aβ capture antibodies used in this study were the monoclonal 6E10 and 4G8, raised against Aβ residues 1–16 and 17–24, respectively (Signet Laboratories, Inc. Dedham, MA). Two polyclonal antibodies recognizing the C-terminal region of Aβ were also utilized, R293 and R309, raised against Aβ residues 32–40 and Aβ residues 34–42 (Dr. P. Mehta, Institute for Basic Research and Mental Disabilities, Staten Island NY). In addition, bovine IgG (Pierce) was used as a negative control. All antibodies were adjusted to 0.5 mg/ml with PBS, loaded in aliquots of 2 μl onto PS20 ProteinChip® arrays, and incubated in a humidity chamber for 2 h at room temperature. The surfaces were blocked with 2 μl of glycine (0.1 M, pH 8.0) for 20 min. After the solutions were removed the spots were washed with 5 μl of 50 mM Tris-HCl, pH 8.0 for 5 min. The chips were washed 2 times with 10 ml of PBS, 0.5% Triton X-100 for 10 min and then twice with 10 ml of PBS for 10 min. A 2-μl sample was loaded, and the chip was incubated in a humidity chamber at 4 °C overnight. After the medium was removed the chips were washed 2 times with 10 ml of PBS-Triton for 10 min, twice with PBS for 10 min, and finally washed 2 times with distilled water and air-dried. A 1:5 dilution of α-cyano-4-hydroxycinnamic acid (5 mg/ml) dissolved in a mixture of 0.1% trifluoroacetic acid in water and acetonitrile (1:1 ratio) was added (2 times, 1-μl each), and mass assignments were made by averaging 100 shots in a Ciphergen Seldi™ Protein Biology System (PBS II). Calibration was externally made with the Ciphergen All-in-1 peptide® standard.

RESULTS

Thioflavine S-stained cerebral cortex sections from human FAD AβPP V717F mutation revealed the presence of numerous cortical plaques composed of flocculent aggregates of amyloid fibrils surrounded by profuse NFT (Fig. 1*A*). Particularly notable was an almost complete absence of the classical amyloid plaque core structures that are commonly observed in sporadic AD individuals who carry the wild-type AβPP gene (Fig. 1*B*). The AβPP V717F mutation produced a moderate amyloid deposition in the leptomeningeal vasculature (Figs. 1, *C* and *D*). Amyloid deposits created in the AβPP V717F mutant individuals were resistant to complete disruption in buffers containing SDS-EDTA, a characteristic shared with the compact amyloid cores of the wild-type Aβ present in sporadic AD patients. The SDS-EDTA buffer efficiently dispersed the flocculent amyloid aggregates into fine bundles recovered by high speed centrifugation that were clearly visible with thioflavine S staining (Fig. 1*E*). From a neuropathological point of view, a striking consequence of the AβPP V717F mutation is the staggering number of NFT, in amounts seldom seen in sporadic AD cases. As demonstrated in Fig. 1*F*, a very rich fraction of SDS-EDTA-insoluble NFT is recovered by low speed centrifugation.

To compare the differences between the amyloid peptides deposited in sporadic AD and AβPP V717F FAD individuals, the amyloid cores present in senile plaques of the former were purified and enriched by stepwise sucrose gradient centrifugations (12). The amyloid cores were solubilized in 80% GDFA and subjected to FPLC size-exclusion chromatography under denaturing conditions (Fig. 2*A*). Most of the dimeric, trimeric, and tetrameric Aβ peptides were cross-linked and oxidized, whereas the monomeric forms were mainly composed of intact and N-terminal-degraded Aβ ending at residues 40 and 42. A high percentage of the Aβ peptides were post-translationally modified (12), and these alterations enhanced their insolubility and resistance to enzymatic degradation (12, 13).

The SDS-EDTA insoluble amyloid derived from the flocculent senile plaques of the AβPP V717F FAD individuals was enriched through a series of high speed centrifugations. Size-exclusion FPLC chromatography produced three large discrete peaks (Fig. 2*B*). Immuno-dot blot indicated that the central broad peak, which included peptides with a M_r of 2.5–9 kDa,

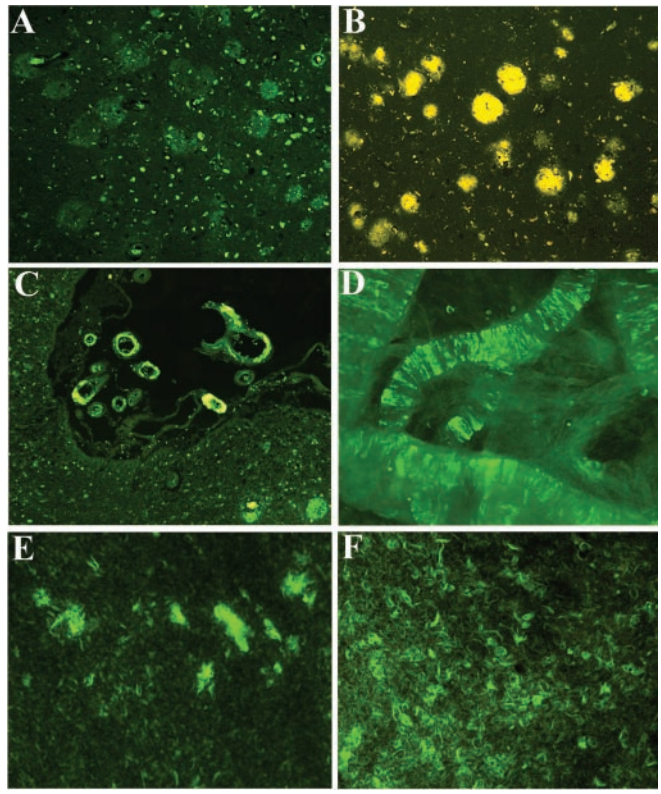

FIG. 1. **Amyloid pathology in FAD and sporadic AD stained by thioflavine S.** *A*, histological section of the cerebral cortex from a patient carrying the AβPP V717F mutation. The numerous and delicate flocculent plaques are composed of fine aggregated amyloid fibrils that almost merge with the neuropil, which contains a large number of neurons with abundant intracellular NFT. *B*, section of the superior frontal gyrus from a sporadic AD patient. Notice the large number of diffuse and mature amyloid plaques. The amyloid fibrils in these plaques are very dense and compact, in contrast to those seen in *A*. *C*, a cross-section of leptomeningeal vessels showing a moderate amount of amyloid deposits. *D*, whole-mount preparation of leptomeningeal vessels depicting moderate amyloid deposits perpendicular to the vessel main axis after the orientation of the smooth muscle cells. *E*, detergent-insoluble fine amyloid aggregates recovered after 275,000 × *g* centrifugation. These amyloid fibrils, which were about 50% pure, were submitted to chromatography to enrich the Aβ peptides and were chemically characterized as described in the text. *F*, abundant NFT were recovered from the detergent-insoluble 135,000 × *g* pellet. Almost every skein of fibrillar material in this fraction represents either neurofibrillary tangles or neuropil threads. Magnifications: *A–D* 100×; *E* and *F* 200×.

contained Aβ peptides (Fig. 2*B*). As can be appreciated in this figure the oligomeric and monomeric Aβ forms were not resolved, suggesting this large fraction contains a complex heterogeneous mixture of hydrophobic peptides of similar molecular M_r. As an alternative to the SDS-EDTA purification protocol, the cerebral cortex of the AβPP V717F mutation was directly lysed in 80% GDFA, and the supernatant was fractionated by FPLC size-exclusion chromatography (Fig. 2*C*). This method yielded a chromatographic profile similar to that of the SDS-EDTA protocol, with most of the Aβ immunopositive reaction localized to the 2.5–9-kDa fractions.

Previous studies of the AβPP V717F individuals demonstrated the presence of Aβ40 and Aβ42 peptides, which were characterized after tryptic-CNBr hydrolysis (17). However, because of their insolubility and tendency to aggregate and precipitate, any native Aβ peptides and C-terminal tryptic peptides longer than 42 residues may be lost during standard HPLC procedures. The chromatographic fractions from patient A, which were separated by C8 reverse-phase HPLC at high temperature (80 °C), were subjected to immuno-dot blot anal-

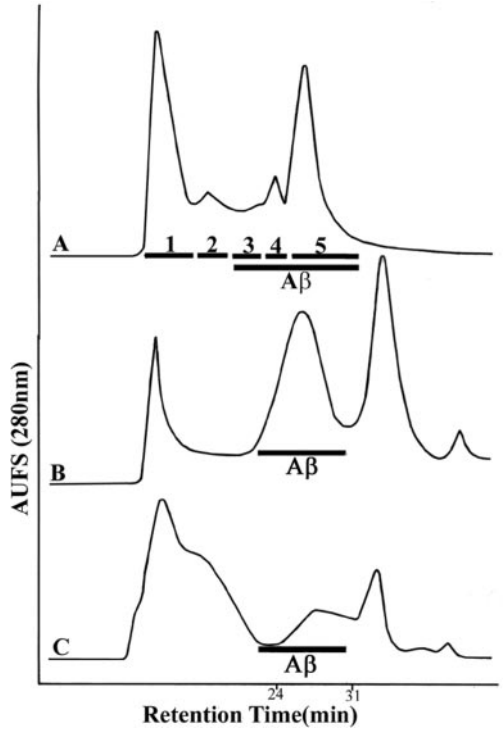

FIG. 2. **Superose 12 FPLC chromatographic profiles of human brain amyloid and crude homogenates.** *A*, chromatographic separation of purified amyloid cores from sporadic AD. Fractions *3*, *4*, and *5* contain tetrameric/trimeric, dimeric, and monomeric Aβ peptides, respectively. Fractions *1* and *2* represent an assortment of insoluble glycolipids and glycoproteins. *B*, chromatographic profile of enriched amyloid from an individual carrying the AβPP V717F FAD mutation. The Aβ peptides are concentrated in the peak *underlined* by a *bar*. As explained in the text this broad peak contains a mixture of complex oligomeric Aβ peptides of different lengths. *C*, chromatographic trace of FAD AD cerebral cortex directly lysed in GDFA. The acid treatment, ultracentrifugation, and size-exclusion column permits the rapid elimination of most of the lipids and insoluble material such as blood vessels, cross-linked collagen, and lipofuscin granules. It also eliminates most of the protein, carbohydrate, and nucleotide molecules and solubilizes the total amount of Aβ present in the cortex and blood vessels which elutes between 24 and 31 min. *AUFS*, arbitrary units full scale.

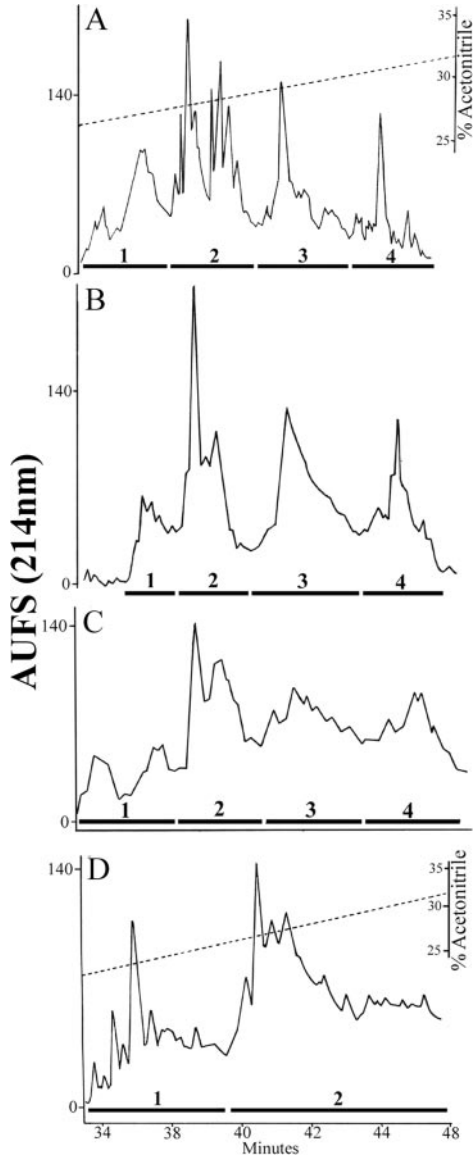

FIG. 3. **Reverse-phase HPLC profiles of Aβ peptides.** *A*, chromatographic separation of the Aβ peptides derived from patient A expressing the AβPP V717F mutation. The collected fractions were pooled into four major groups as indicated by the *horizontal bars* and submitted to MALDI-TOF mass spectrometry for identification. The *hyphenated line* indicates the elution concentration of acetonitrile, which was the same for *B* and *C*. *B*, elution pattern generated by the Aβ peptides derived from V717F mutant patient B. Notice that the distribution and shape of the Aβ peptides is different from that of patient A, probably due to individual variations in rate of synthesis, incorporation into filaments, and differences in degradation in addition to other phenotypic disparities. *C*, HPLC profile of the human wild-type AβPP-Aβ-derived peptides. The chromatography was developed under the same conditions as illustrated for *A* and *B*. The analysis of this specimen, which also showed a complex mixture of Aβ peptides, has been published (12). Most of this complexity is due to N-terminal degradations of the Aβ peptides. *D*, chromatographic trace of Aβ peptides extracted from the leptomeningeal vessels of the AβPP V717F mutation from patient C. The chromatographic profile and Aβ peptide composition of the vascular deposits largely deviates from those observed for the parenchymal plaque deposits. *AUFS*, arbitrary units full scale.

yses using Aβ 4G8 and 6E10 antibodies. This experiment revealed that the Aβ peptides were spread in an incompletely resolved section of the C8 reverse-phase chromatography encompassing four consecutive, large fractions (Fig. 3*A*). These fractions were submitted to mass spectrometry analysis and revealed a complex mixture of Aβ peptide species (Table I). The spontaneous cyclization of Glu-3 and Glu-11 at the N-terminal position resulted in pyroglutamyl residues, a modification commonly observed in the wild-type Aβ peptides. The N- and C-terminal regions were heterogeneous with Aβ peptides starting at residues Asp-1, Asp-2, Glu-3, Phe-4, Arg-5, His-6, Asp-7, Gly-9, Tyr-10, Glu-11, His-13, His-14 and ending at Aβ residues Val-36, Gly-37, Gly-38, Val-39, Val-40, Ile-41, Ala-42, Val-44, Val/Phe-46, Thr-48, Leu-49, and Val-50 (Table I).

To confirm that the C-terminal region of the AβPP V717F-derived Aβ peptides extended beyond the wild-type Aβ40 and Aβ42 termini, peaks 1–4 of the C8 HPLC-separated fractions (Fig. 3*A*) were subjected to tryptic (Tp) hydrolysis followed by cyanogen bromide (CNBr) cleavage. The Tp-CNBr resulting peptides were separated by C18 reverse-phase HPLC in the presence of a linear gradient formed by water/acetonitrile-isopropanol. We concentrated our initial efforts on C8 HPLC fractions 2 and 3 (Fig. 3*A*) since previous studies demonstrated the retention time corresponded to the elution of Aβ 1–40 and 1–42 peptides (14). As can be appreciated in Fig. 4, this chromatography was capable of resolving the Tp-CNBr-hydrolyzed Aβ peptides of up to 42 amino acid residues (Fig. 4). However, also present was a broad unresolved fraction of larger hydrophobic Aβ-related peptides that MALDI-TOF mass spectrometric analysis revealed as residues starting at 17, 29, and 36 and terminating at residues beyond amino acid 42. We then exam-

TABLE I
Aβ-related peptides (MALDI-TOF)

PG, pyroglutamyl; f, + 1 formyl (M_r + 28); 2f, +2 formyl (M_r + 56): O, +1 oxygen (M_r + 16).

Observed M_r	Calculated M_r	Peptide
Peak 1		
2951.8	2952.4	13–40 + f
3831.5	3832.3	3–36
4326.7	4326.9	3PG-42 + O
4346.2	4346.9	1–40 + O
4974.8	4975.7	1–46 (Phe)
5381.6	5382.2	1–50 + f
Peak 2		
3388.6	3388.9	9–40 + O
3817.6	3817.3	4–38
3899.1	3899.4	3PG-37 + f
3917.1	3916.5	4–39
3929.7	3928.4	3PG-38
4015.4	4015.6	4–40
4081.9	4080.6	5–42 + f
4229.3	4227.8	4–42 + f
4275.2	4275.7	1–39 + f + O
4328.4	4328.9	3–42
5051.1	5050.9	3PG-49
Peak 3		
2788.0	2787.3	14–40
3334.7	3334.9	11PG-42 + O
3817.5	3817.3	4–38
4047.0	4046.5	1–36 + f
4232.0	4231.8	2–40 + O
4286.2	4285.9	3–41 + f
4511.3	4511.2	3PG-44
4512.0	4511.2	3PG-44
4600.6	4600.3	2–44
4982.2	4983.7	3–48 + f
5154.6	5154.9	3PG-49(Phe-46) + 2f
Peak 4		
3316.2	3315.9	10–40
3319.2	3318.9	11PG-42
3427.9	3428.9	9–40 + 2f
3499.3	3500.1	10–42
3555.7	3556.1	10–42 + 2f
3758.4	3759.3	7–42
3897.4	3898.5	6–42
4300.4	4300.9	4–43
4310.2	4310.9	3PG-42
4512.4	4511.2	3PG-44
4722.8	4723.5	3PG-46
5018.3	5019.7	1-46 (Phe-46) + f + O
5418.1	5418.2	1-50 (Phe-46) + O

ined the Tp-CNBr-hydrolyzed peptides of the HPLC-separated fractions 1–4 (Fig. 3*A*) by MALDI-TOF mass spectrometry. A series of Aβ-related peptides were identified that started at residues Glu-3, His-6, Leu-17, Gly-29, and Leu-36 and ending, as expected, at residues Arg-5, Lys-16, Lys-28, homoserine (Hse) 35, Val-40, and Ala-42 (Table II). In addition, MALDI-TOF mass spectrometry also detected hydrophobic peptides ending at residues homoserine lactone 35 (>Hse), Ile-41, Thr-43, Val-44, Ile-45, Val/Phe-46, Ile-47, Thr-48, Leu-49, Val-50, Met-51, and Leu-52 (Table II).

For the characterization of the Aβ peptides isolated from patient B, the C8 reverse-phase HPLC fractions 1–4 (Fig. 3*B*) were analyzed by SELDI-TOF mass spectrometry. Four different anti-Aβ antibodies were used independently to capture the Aβ-related peptides, 4G8, 6E10, R293, and R309 (the binding specificities of these antibodies are described under "Materials and Methods"). The Aβ-related peptides in patient B also represented a heterogeneous mixture initiating at residues Asp-1, Asp-2, Glu-3 (and its derivative, pyroglutamyl), Phe-4, and Leu-17 and ending at residues Gly-37, Gly-38, Val-40, Ile-41, Ala-42, Thr-43, Val-44, Ile-45, Thr-48, Val-50, and Lys-54 (Table III). These peptides were localized in fractions 2–4. The peptides in fraction 1 were insufficient to permit M_r assign-

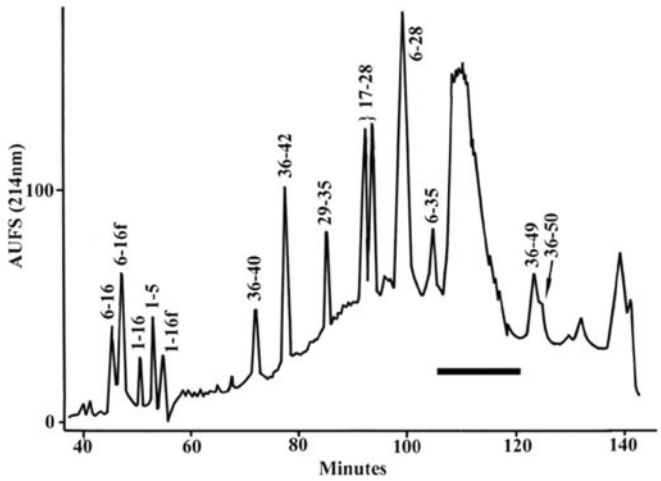

FIG. 4. **Chromatographic profile of tryptic-CNBr peptides.** This hydrolysate was derived from fractions 2 and 3 shown in Fig. 3*B*. Automatic amino acid analysis revealed, as expected, Aβ peptides ending in Arg-5, Lys-16, Lys-28, or Met-35. The fraction containing the Aβ peptide residues 17–28 appeared as a double peak. Both peaks had the same atomic mass, suggesting either racemization of Ser-26 or isomerization of Asp-23, which commonly occur in the human Aβ peptides (12, 31). Between 107–120 min retention time there was a broad peak, indicated by the *horizontal bar*, which contained a complex mixture of unresolved hydrophobic and aggregated Aβ-derived peptides apparently starting at residues Leu-17, Gly-29, and Leu-36 and probably ending at residues beyond Ala-42, which could not be clearly resolved by amino acid analysis. The chromatography also suggests that the amount of Aβ ending at Ala-42 is more abundant than that ending at residue Val-40. *AUFS*, arbitrary units full scale.

ments. All antibodies, including those raised against the C-terminal regions of the Aβ wild-type peptides ending at residues Val-40 and Ala-42 (Arg-293 and Arg-309) captured the Aβ peptides ending at residues Gly-37, Gly-38, Ile-41, Thr-43, Val-44, Ile-45, Thr-48, Val-50 (Table III). Most of the Aβ peptides residues ending in Val-40 and Ala-42 were in fraction 2 (Fig. 3*B*), although these peptides were also present in fractions 3 and 4. The wide spread of Aβ peptides with the same or similar sequences among the HPLC fractions may be explained in terms of the enormous ability of Aβ to associate into dimers, trimers, or tetramers that increase retention time.

For comparison, the C8 reverse-phase chromatographic profile of the human wild-type peptides is shown in Fig. 3*C*. The mass spectrometry of these peptides has been published (14). In the amyloid deposits obtained from sporadic AD, no peptides longer than 40 and 42 amino acids were recovered. The complexity of the chromatographic pattern is largely due to the extensive degradation of the Aβ40 and Aβ42 peptides and to post-translational modifications.

To characterize the Aβ peptides present in vascular amyloid deposits of the AβPP V717F mutation, the leptomeningeal vessels were dissected from the arachnoid membranes of patient C, treated with GDFA and the supernatant submitted to FPLC and C8 reverse-phase HPLC (Fig. 3*D*). SELDI-TOF mass spectrometry using the 6E10 antibody (against Aβ residues 1–16) revealed that the group of peptides with early retention time contained shorter Aβ sequences (Table IV). These peptides started at residue Asp-1 and ended at residues Glu-22, Asp-23, Val-24, Gly-25, and Ser-26 as well as at residues Ala-30 and Ile-31 (Table IV). In addition, the longer and relatively insoluble Aβ peptides with C termini at residues Gly-38, Val-39, Val-40, Ala-42, and Val-44 (Table IV) appear to be the major components of the vascular amyloid in the AβPPV717F mutant. We did not detect Aβ peptides longer than 44 residues, perhaps because their insolubility hindered diffusion into the vascular spaces or because they were readily entrapped and

TABLE II
Tryptic and CNBr peptides (MALDI-TOF)

a, +1 formyl (M_r + 28); b, +2 formyl (M_r + 56); c, +1 oxygen (M_r + 16); d, +2 oxygen (M_r + 32); e, +met → homoserine; f, +met → homoserine lactone; PG, pyroglutamyl.

Observed M_r	Calculated M_r	Peptide
1840.7	1841.0	2–16 (b)
433.7	433.5	3PG-5
1808.0	1807.9	3PG-16b
3713.6	3713.1	3–35 f + a
4923.1	4922.7	6–51(Phe-46) f + b
1934.2	1934.3	17–35 f
2680.2	2679.2	17–43
2466.0	2465.9	17–40 b + c
2582.9	2563.0	17–41 b
3062.8	3062.6	17–46 b + c
3563.7	3564.3	17–51 (Phe-46) f + c
3752.7	3753.6	17–52 (Phe-46) a + c
3706.2	3705.8	17–52 a + c
645.9	644.8	29–35 e
1227.8	1227.6	29–41 a (c)
1270.8	1270.6	29–42 (a + c) (b) (b + c)
1471.8	1470.9	29–44 (a + c)
1710.3	1711.2	29–46 a (a + c)
1787.2	1787.2	29–48 (Phe-46) b (a + c)
1845.1	1844.3	29–47 (Phe-46) (a) (c) (a + c) (b + c)
1897.8	1897.4	29–48
2113.8	2114.6	29–49 (Phe-46)b
2153.9	2153.7	29–50 a + c
2376.9	2376.9	29–51 (Phe-46) b + d
2462.4	2462.1	29–52 (Phe-46) a + d (c)
669.9	670.8	36–42 b (a)
983.6	984.2	36–46b
1075.0	1075.3	36–46 (Phe-46)
1168.0	1168.5	36–47 a
1289.9	1289.6	36–48 (Phe-46)
1430.1	1430.7	36–49 (Phe-46)a
1411.2	1410.7	36–49b
1501.0	1501.9	36–50 (Phe-46) a
1661.3	1661.1	36–51 (Phe-46) a (c) (e) (f + b)
1698.4	1698.2	36–52 (a) (b) (c)
1790.0	1790.2	36–52 (Phe-46) a + c (b + c)

incorporated into the insoluble amyloid fibrils of the flocculent senile plaques of the cerebral cortex.

DISCUSSION

We characterized the Aβ peptides present in the brain parenchyma and leptomeningeal vessels of three FAD individuals carrying the AβPP V717F mutation to compare them to the Aβ peptides characteristic of sporadic AD patients. Our experiments reveal that significant differences exist between the amyloid deposited in these rare FAD individuals and those considered characteristic for sporadic AD. The longer and more hydrophobic Aβ peptides produced by V717F mutation polymerize into fine bundles of detergent-insoluble amyloid fibrils and eventually organize into flocculent spherical aggregates that dominate the cerebral cortex pathology. For reasons still unclear, these longer Aβ peptides are less inclined to condense into the compact amyloid cores observed in sporadic AD. The amount of amyloid deposited in the leptomeningeal and parenchymal arteries in the V717F individuals was moderate and does not appear to grossly differ from that observed in the sporadic AD cases possessing the apolipoprotein E ϵ3 genotype.

Extending the Aβ sequence at the C terminus beyond residue Aβ42 will result in more hydrophobic Aβ peptides since this sequence is part of the mostly non-polar AβPP transmembrane sequence of 24 amino acids, ^{29}GAIIGLMVGGVVIATVIVITLVML[52]. It has been suggested that to generate amyloid fibrils, the wild-type Aβ C-terminal hydrophobic domains (residues 29–42) organize into helical stacks of hydrophobic β-sheets. These antiparallel β-sheets, which are perpendicular to the filament main axis, are stabilized by hydrogen bonds parallel to the main axis of the filament and are shielded from the surrounding water by the mostly polar Aβ sequence of residues 1–28 (15, 16). A longer non-polar C terminus may result in a

TABLE III
Aβ related peptides (SELDI-TOF)

PG, pyroglutamyl; O, + 1 oxygen (M_r + 16); f, + 1 formyl (M_r + 28); 2f, +2 formyl (M_r + 56).

Antibody Peak	Observed M_r	Calculated M_r	Peptide
6E10/2	3905.0	3905.4	3–37 + O
	3936.6	3933.4	3–37 + f + O
	4332.5	4330.9	1–40
	4517.1	4515.1	1–42
	4533.2	4531.1	1–42 + O
4G8/2	4331.3	4330.9	1–40
	4533.9	4531.1	1–42 + O
	3968.2	3965.9	17–54 (Phe)
	5447.9	5446.2	1–50 (Phe) + f + O
R293/2	3906.1	3905.4	3–37 + O
	3938.0	3933.4	3–37 + f + O
	4332.0	4330.8	1–40
	4534.7	4531.1	1–42 + O
R309/2	3906.1	3905.4	3–37 + O
6E10/3	4312.5	4313.9	3–41
	4372.8	7372.9	3–42 + O
4G8/3	3965.1	3965.9	17–54 (Phe)
	4304.8	4300.9	2–44
	4202.3	4200.7	3–40 + f + O
	5446.8	5446.2	1–50 (Phe) + f + O
6E10/4	4313.8	4313.9	3–41
	4356.9	4356.9	3–42 + f + O
	4475.1	4474.0	4–43 + f + O
	4601.3	4600.3	2–44
	4618.3	4616.3	2–44 + O
	4833.0	4632.2	1–43 + O
4G8/4	4312.3	4313.9	3–41
	4356.9	4356.9	3–42 + f + O
	4602.7	4600.3	2–44
	4618.8	4616.2	1–43
	4634.1	4832.2	1–43 + O
R293/4	4314.0	4313.9	3–41
	4603.3	4600.3	2–44
	4711.2	4713.4	2–45
	5032.9	5031.8	3–48 (Phe) + f
	5431.4	5430.2	1–50 (Phe) + f
R309/4	3978.8	3974.4	3–38
	4358.9	4356.9	3–42 + f + O
	4445.9	4446.0	3–43 + O
	4475.1	4474.0	3–43 + f + O
	4587.3	4585.2	3–44 + 2f
	4601.8	4600.3	2–44
	4619.5	4616.3	2–44 + O
	4732.9	4729.4	2–45 + O
	5028.8	5029.8	3(PG)-48(Phe) + f + O

TABLE IV
Aβ-related peptides (SELDI-TOF) captured by 6E10

O, + 1 oxygen (M_r + 16); 2f, 2 formyl (M_r + 56).

Observed M_r	Calculated M_r	Peptide
2662.9	2661.9	1–22
2778.5	2777.0	1–23
2876.9	2876.1	1–24
2934.6	2933.2	1–25
3018.9	3020.2	1–26
3445.5	3446.6	1–30
3519.2	3519.8	1–31 + O
4150.3	4148.6	1–38
4148.7	4148.6	1–38 + O
4234.9	4231.7	1–39
4331.0	4330.9	1–40
4349.0	4346.9	1–40 + O
4517.7	4515.1	1–42
4534.4	4531.1	1–42 + O
4388.2	4386.9	1–40 + 2f
4218.7	4215.8	2–40
4418.2	4416.1	4–44 + O

more stable and hydrophobic core and a molecule that is more insoluble and prone to polymerize into amyloid filaments.

The presence of the AβPP V717F substitution may interfere with γ-secretase cleavage at either Val-40 or Ala-42 and, thus, permit the generation of longer Aβ peptides ending at residues from Thr-43 to Lys-54. Alternatively, carboxypeptidases could have degraded the longer Aβ to sequentially generate shorter Aβ peptides. In support of this last hypothesis is immunocytochemical evidence showing that in AD, several lysosomal proteases with endo-, amino-, and carboxypeptidase activity are abundantly associated with the AD amyloid deposits (17, 18). These enzymatic activities are not observed in control brain tissue in which the neuritic amyloid plaques are virtually absent, lending support to an *in vivo* Aβ degradation in the AD brain. In addition, cathepsin D has been found to degrade longer recombinant AβPP peptides at position Aβ-(Leu-49–Val-50) (19), and in cell cultures there is evidence for the presence of an ϵ-secretase that generates small quantities of longer Aβ peptides ending at residue Leu-49 (20). However, we cannot rule out the possibility of some postmortem artifactual degradation of longer Aβ peptides by lysosomal enzymes in the case of the AβPP V717F patient brain, which is never observed in sporadic AD. Interestingly, the three individuals carrying the AβPP V717F mutation developed their amyloid deposits and ensuing dementia about 2–3 decades earlier than the average of those with sporadic AD that bear the wild-type AβPP. Furthermore, these patients also have on the average a substantially shorter disease course. Whether the enzymatic activity involved in the generation of the Aβ peptides is due to ϵ- or γ-secretase or cathepsin activity, the presence of these longer peptides in individuals carrying the AβPPV717F mutant contributes to the premature AD onset and death of these patients. Furthermore, it has been suggested that there is a pathophysiological relationship between amyloid and NFT production (21). The presence of AβPP V717F mutation ultimately results in massive NFT generation, which may also contribute to the earlier death of these FAD patients.

In addition to the longer Aβ peptides and those ending at positions 40 and 42, several longer Aβ peptides starting at position Leu-17 (the α-secretase cleavage site is between residues Lys-16 and Leu-17) were also recovered in the brains of AβPP V717F FAD patients. In AD, the peptide 17–42 has been recovered from diffuse plaques and is apparently not associated with neuritic pathology or microglia activation. This non-fibrillar peptide deposits into diffuse amorphous aggregates, suggesting that the N-terminal region of Aβ (residues 1–16) is essential for fibrillogenesis (22). It is possible that in the AβPP V717F individuals peptides starting at residue 17 and extending longer than residue 42 may contribute to AD pathology. Future studies will be necessary to clarify the potential pathological activity of these peptides. Another important N-terminal-truncated peptide to be considered is that starting at Aβ residue Glu-11 and ending at Ala-42. Upon the enzymatic characterization of the β-secretase it was found that this enzyme, besides cleaving the AβPP between residues −1 Met and +1 Asp (Aβ numbering), is also capable of hydrolyzing the peptide bond between Tyr-10 and Glu-11 (23).

The use of GDFA as a solubilizing and disaggregating agent produced artifactual formylation of N termini and hydroxyamino acids. There were numerous instances in which the Aβ peptides were oxidized at Met-35 to Met sulfone and Met sulfoxide (Tables I-III). We suggest that some of these oxidations may have actually occurred *in vivo* and contribute to the insolubility of Aβ peptides and blocked CNBr cleavage (13). The human wild-type Aβ peptides present in the sporadic AD cases are heavily altered post-translationally at residues 1 and 7, where the Asp residues are modified to Iso-Asp, resulting in the formation of β-shifts (12). In this instance the peptide bond is formed between the β carbon of Asp and the α-amino group of the subsequent amino acid with no alterations in M_r. Because of the relatively small amounts of available FAD patient tissue we were unable to undertake a search for these modifications, although it can be assumed that some of these isomers also exist in the mutant AβPP V717F amyloid deposits.

The best understood precipitating pathological mechanisms in FAD appear to be directly related to mutations that increase Aβ synthesis, such as the double Aβ flanking mutations K670N and M671L ($A\beta PP_{770}$ numbering). These mutations boost β-secretase cleavage, an event that apparently promotes γ-secretase hydrolysis and increases Aβ production (24). Those AβPP mutations affecting the Aβ peptide middle domain such as E693Q, E693G, E693K, and D694N ($A\beta PP_{770}$ numbering) alter Aβ conformation and loss of electrostatic repulsion with the negatively charged glycosaminoglycans, resulting in an overwhelming amount of vascular amyloid deposition (25, 26).

The chemical characterization of Aβ peptides produced by other FAD AβPP mutations distal to the Aβ40 and Aβ42 residues, such as V715M, I716V, V717I, V717G, and L723P ($A\beta PP_{770}$ numbering) (2), all capable of producing dementia, awaits further investigation. The production of longer Aβ peptides has been observed previously. Several laboratories report small quantities of longer Aβ species ending at residue Leu-49 (Aβ numbering), which corresponds to the S3 cleavage site of Notch-1 (20, 27, 28). Human skeletal muscle, besides generating Aβ40 and Aβ42, also produces small quantities of Aβ ending at residues Val-44, Ile-45, and Val-46 (29).

In summary, the FAD AβPP V717F amino acid substitution results in the production of an early onset and aggressive dementia. Biochemical examination of three FAD cases revealed that a unique and complex Aβ peptide species array was produced in these individuals. Our experiments revealed that structural heterogeneity exists between the Aβ peptides produced in three individuals from this single FAD kindred. In addition, the amyloid deposits created in this FAD kindred differ substantially from those characteristic of sporadic AD. Although the PDAPP Tg mice constructed to overexpress this mutant Aβ clearly mimic many AD aspects of the amyloid cascade, our experiments reveal that it is important to consider that these animals probably do not exactly reproduce the biochemical features associated with the sporadic human form of the disease. Previous experiments with other transgenic mice carrying the human Swedish mutations (K670N, M671L) driven by the Thy-1 (APP23) or the hamster prion (tg2576) promoters reveal that the accumulated amyloid, although structurally similar, is not biochemically equivalent to that deposited in sporadic AD patients (30). Rather, it is probably best to remain cognizant that sporadic AD amyloid accumulation results from multiple inherited and environmental factors acting in concert over extended periods, a situation that is not duplicated in either FAD patients or transgenic mice.

REFERENCES

1. Mirra, S. S., and Hyman, B. T. (2002) in Greenfield's Neuropathology (Graham, D. I., and Lantos, P. L., eds) Vol. II, pp. 195–272, Arnold, New York
2. Miravalle, L., Tokuda, T., Chiarle, R., Giaccone, G., Bugiani, O., Tagliavini, F., Frangione, B., and Ghiso, J. (2000) *J. Biol. Chem.* **275,** 27110–27116
3. Selkoe, D. J. (2001) *Physiol. Rev.* **81,** 741–766
4. Selkoe, D. J. (1997) *Science* **275,** 630–631
5. Murrell, J., Farlow, M., Ghetti, B., and Benson, M. D. (1991) *Sci.* **254,** 97–99
6. Farlow, M., Murrell, J., Ghetti, B., Unverzagt, F., Zeldenrust, S., and Benson, M. (1994) *Neurology* **44,** 105–111
7. Ghetti, B., Murrell, J., Benson, M. D., and Farlow, M. (1992) *Brain Res.* **571,** 133–139
8. Games, D., Adams, D., Alessandrini, R., Barbour, R., Berthelette, P., Blackwell, C., Carr, T., Clemens, J., Donaldson, T., Gillespie, F., Guido, T., Hagopian, S., Johnson-Wood, K., Khan, K., Lee, M., Leibowitz, P.,

Lieberburg, I., Little, S., Masliah E., McConlogue, L., Montoya-Zavala, M., Mucke L., Paganini, L., Penniman, E., Power, M., Schenk D., Seubert, P., Snyder, B., Soriano, F., Tan, H., Vitale, J., Wadsworth, S., Wolozin, B., and Zhao, J. (1995) *Nature* **373,** 523–527
9. Schenk, D., Barbour, R., Dunn, W., Gordon, G., Grajeda, H., Guido, T., Hu, K., Huang, J., Johnson-Wood, K., Khan, K., Kholodenko, D., Lee, M., Liao, Z., Lieberburg, I., Motter, R., Mutter, L., Soriano, F., Shopp, G., Vasquez, N., Vandevert, C., Walker, S., Wogulis, M., Yednock, T., Games, D., and Seubert, P. (1999) *Nature* **400,** 173–177
10. Masliah, E., Sisk, A., Mallory, M., Mucke, L., Schenk, D., and Games, D. (1996) *J. Neurosci.* **16,** 5795–5811
11. Weller, R. O., Massey, A., Newman, T. A., Hutchings, M., Kuo, Y. M., and Roher, A. E. (1998) *Am. J. Pathol.* **153,** 725–733
12. Roher, A. E., Lowenson, J. D., Clarke, S., Wolkow, C., Wang, R., Cotter, R. J., Reardon, I. M., Zurcher-Neely, H. A., Heinrikson, R. L., Ball, M. J., and Greenberg, B. D. (1993) *J. Biol. Chem.* **268,** 3072–3083
13. Kuo, Y. M., Emmerling M. R., Woods, A. S., Cotter, R. J., and Roher A. E. (1997) *Biochem. Biophys. Res. Commun.* **237,** 188–191
14. Kalback, W., Watson, M. D., Kokjohn, T. A., Kuo, Y. M., Weiss, N., Luehrs, D. C., Lopez, J., Brune, D., Sisodia, S. S., Staufenbiel, M., Emmerling, M., and Roher, A. E. (2002) *Biochem.* **41,** 922–928
15. Lansbury, P. T., Jr., Costa, P. R., Griffiths, J. M., Simon, E. J., Auger, M., Halverson, K. J., Kocisko, D. A., Hendsch, Z. S., Ashburn, T. T., Spencer, R. G., Tidor, B., and Griffin, R. G. (1995) *Nat. Struct. Biol.* **2,** 990–998
16. Chaney, M. O., Webster, S. D., Kuo, Y. M., and Roher, A. E. (1998) *Protein Eng.* **11,** 761–767
17. Cataldo, A. M., and Nixon, R. A. (1990) *Proc. Natl. Acad. Sci. U. S. A.* **87,** 3861–3865
18. Cataldo, A. M., Paskevich, P. A., Kominami, E., and Nixon, R. A. (1991) *Proc. Natl. Acad. Sci. U. S. A.* **88,** 10998–11002
19. Higaki, J., Catalano, R., Guzzetta, A. W., Quon, D., Nave, J. F., Tarnus, C., D'Orchymont, H., and Cordell, B. (1996) *J. Biol. Chem.* **271,** 31885–31893
20. Weidemann, A., Eggert, S., Reinhard, F. B., Vogel, M., Paliga, K., Baier, G., Masters, C. L., Beyreuther K., and Evin, G. (2002) *Biochemistry* **41,** 2825–2835
21. Hardy, J., and Selkoe, D. J. (2002) *Science* **297,** 353–356
22. Gowing, E., Roher A. E., Woods, A. S., Cotter, R. J., Chaney, M., Little, S. P., and Ball, M. J. (1994) *J. Biol. Chem.* **269,** 10987–10990
23. Vassar, R., Bennett, B. D., Babu-Khan, S., Kahn, S., Mendiaz, E. A., Denis, P., Teplow, D. B., Ross, S., Amarante, P., Loeloff, R., Luo, Y., Fisher, S., Fuller, J., Edenson, S., Lile, J., Jarosinski, M. A., Biere, A. L., Curran, E., Burgess, T., Louis, J. C., Collins, F., Treanor, J., Rogers, G., and Citron, M. (1999) *Science* **286,** 735–741
24. Sinha, S., and Lieberburg, I. (1999) *Proc. Natl. Acad. Sci. U. S. A.* **96,** 11049–11053
25. Watson, D. J., Lander, A. D., and Selkoe, D. J. (1997) *J. Biol. Chem.* **272,** 31617–31624
26. Castillo, G. M., Lukito, W., Wight, T. N., and Snow, A. D. (1999) *J. Neurochem.* **72,** 1681–1687
27. Sastre, M., Steiner, H., Fuchs, K., Capell, A., Multhaup, G., Condron, M. M., Teplow, D. B., and Haass C. (2001) *EMBO Rep.* **2,** 835–841
28. Gu, Y., Misonou, H., Sato, T., Dohmae, N., Takio, K., and Ihara, Y. (2001) *J. Biol. Chem.* **276,** 35235–35238
29. Kuo, Y. M., Kokjohn, T. A., Watson, M. D., Woods, A. S., Cotter, R. J., Sue, L. I., Kalback, W. M., Emmerling M. R., Beach T. G., and Roher A. E. (2000) *Am. J. Pathol.* **156,** 797–805
30. Kuo, Y. M., Beach, T. G., Sue, L. I., Scott, S., Layne, K. J., Kokjohn, T. A., Kalback, W. M., Luehrs, D. C., Vishnivetskaya, T. A., Abramowski, D., Sturchler-Pierrat, C., Staufenbiel, M., Weller, R. O., and Roher, A. E. (2001) *Mol. Med.* **7,** 609–618
31. Shimizu, T., Watanabe, A., Ogawara, M., Mori, H., and Shirasawa, T. (2000) *Arch. Biochem. Biophys.* **381,** 225–234